J. Membrane Biol. 196, 147–155 (2003)
DOI: 10.1007/s00232-003-0632-0

The Journal of
Membrane
Biology

Passive Transport of Macromolecules through *Xenopus laevis* Nuclear Envelope

K. Enss, T. Danker, A. Schlune, I. Buchholz, H. Oberleithner
Institute of Physiology I, Nanolab, University of Münster, D-48149 Münster, Germany

Received: 7 May 2003/Accepted: 5 September 2003

Abstract. Although nuclear pore complexes (NPC) are considered to be key structures in gene expression, little is known about their regulatory control. In order to explore the regulatory mechanism of passive transport of small macromolecules we examined the influence of different factors on the diffusional pathway of NPCs in isolated *Xenopus laevis* oocyte nuclei. Diffusion of fluorescence-labeled 10-kD dextran was measured across the nuclear envelope with confocal fluorescence microscopy. Surprisingly, the filling state of the perinuclear Ca^{2+} store had no influence on passive transport of 10-kD dextran. Furthermore, nuclear envelope permeability was independent of cytoplasmic pH (pH range 8.3–6.3). In contrast, nuclear swelling, induced by omission of the endogenous cytosolic macromolecules, clearly increased nuclear permeability. An antibody against the glycoprotein gp62, located at the central channel entrance, reduced macromolecule diffusion. In addition, nuclei from transcriptionally active, early developmental stages (stage II) were less permeable compared to transcriptionally inactive, late-developmental-stage (stage VI) nuclei. In stage II nuclei, atomic force microscopy disclosed NPC central channels with plugs that most likely were ribonucleoproteins exiting the nucleus. In conclusion, the difference between macromolecule permeability and previous measurements of electrical resistance strongly indicates separate routes for macromolecules and ions across the nuclear envelope.

Key words: Nuclear pore complex — Peripheral channels — Nuclear pore plugging — Perinuclear Ca^{2+} store — Oocyte development

Correspondence to: H. Oberleithner; email: oberlei@uni-muenster.de

Introduction

Active and passive transport of various cargo including inorganic ions into and out of the cell nucleus are mediated by nuclear pore complexes (NPCs), supramolecular structures that span the nuclear envelope (NE). As a transport machinery the NPC plays a crucial role in the regulation of gene expression. Structural and functional data indicate the existence of eight small peripheral channels that penetrate individual NPCs around the large central channel (Aebi et al., 1992; Hinshaw et al., 1992; Mazzanti et al., 2001; Shahin et al., 2001).

Electrophysiological methods, such as microelectrode techniques (Loewenstein & Kanno, 1963), the patch-clamp technique (Mazzanti et al., 1990; Bustamante et al., 1995a) and the nuclear hourglass technique (Danker et al., 1999) addressed passive ion transport of the NE. Since the NE is assumed to be a smart barrier that adjusts its permeability to the metabolic demands of the cell (Mazzanti, Bustamanta & Oberleithner, 2001) it seems crucial to understand the regulatory mechanisms of passive macromolecule transport. Functional data should allow conclusions on the conformational state of the NPCs and thus fuse functional and structural data on NPCs into a more universal model.

Superfusion of isolated nuclei with fluorescence-labeled dextran of defined size and application of confocal fluorescence microscopy allow measurements of the passive NE permeability with reasonable precision. We used 10-kD dextran, which is too large to penetrate the small peripheral channels but freely diffuses through open NPC central channels. This technique was used to identify factors that could modify the NPC permeability for small macromolecules.

Since both calcium and ATP affect ion permeability (Mazzanti, Innocenti & Rigatelli, 1994; Shahin et al., 2001) and NPC conformation (Perez-Terzic et al., 1996; Rakowska et al., 1998), we examined the

influence of cisternal calcium on the NPC permeability for small macromolecules. We also explored the influence of pH changes on NE macromolecule-permeability since pH effects of the NE have been reported (Danker & Oberleithner, 2000; Oberleithner et al., 2000a). Nuclear swelling induced by changing osmolarity was already used to elucidate aspects about NE ion-permeability (Innocenti & Mazzanti, 1993). Therefore, we measured passive NE macromolecule-permeability in volume-expanded nuclei.

Individual NPCs consist of more than 100 nucleoporins. Due to its location, one of the nucleoporins, namely the glycoprotein gp62, is of special interest when exploring passive macromolecule transport. The glycoprotein gp62 is part of the so-called gp62 complex located near the central NPC channel (Guan et al., 1995). Although the role of the gp62 complex for active transport has already been elucidated (Finlay et al., 1991; Hu et al., 1996), little is known about its influence on passive transport. The influence of antibodies directed against nucleoporins on NE ion permeability is still controversial (Bustamante, Hanover & Liepins, 1995b; Danker et al., 1999). We used gp62 antibodies to occlude NPC central channels and thus to affect passive macromolecule transport. Finally, structural and functional data indicate transient NPC channel plugging during macromolecule translocation (Oberleithner et al., 2000b; Oberleithner et al., 2001; Schafer et al., 2002). Thus, to explore the possible influence of NPC channel plugging caused by ribonucleoprotein export as reported previously (Schafer et al., 2002), we performed experiments in transcriptionally active (stage II) and transcriptionally inactive (stage VI) *Xenopus laevis* oocytes.

Materials and Methods

Preparation of Cell Nuclei

Female *Xenopus laevis* were anaesthetized with 0.1% tricanemethane sulfonate and their ovaries were removed. Oocytes were dissected from ovary clusters and stored in modified Ringer solution (in mM: 87 NaCl, 3 KCl, 1 $MgCl_2$, 1.5 $CaCl_2$, 10 HEPES, 100 U/100 μg penicillin/streptomycin, pH 7.4) before use. The nuclear isolation medium (NIM) was composed of (in mM): 90 KCl, 26 NaCl, 2 $MgCI_2$, 1.1 EGTA, 10 HEPES. We applied an ATP-regenerating system (3 mM ATP, 3 mM creatine phosphokinase, 10 mM phosphocreatine), free Ca^{2+} (10^{-8}–10^{-5} M, ambient between pH 6.3–8.3 and 1.5% polyvinylpyrrolidone(PVP; M_r = 40,000), as appropriate.

Ca^{2+} Store Depletion

Nuclear Ca^{2+} stores were depleted by incubating isolated nuclei in NIM either containing 50 μM of the membrane-permeable Ca^{2+} chelator BAPTA-AM (BAPTA-AM/DMSO-stock solution: 50 mM) or 1 μM of the Ca^{2+}-channel activator IP_3 (inositol-1,4,5-trisposphate), or by removing ambient Ca^{2+} and/or ATP.

Changes in pH

To test nuclei under three different pH values we titrated the NIM with KOH to a pH of 7.3, 6.3 or 8.3. The first experimental series was performed with an NIM containing a Ca^{2+} concentration of 10^{-7} M and 3 mM ATP (filled Ca^{2+} store). Ca^{2+}-store depletion was induced by removal of ATP and reduction of free Ca^{2+} to 10^{-8} M.

Nuclear Swelling

PVP is needed to compensate for the lack of macromolecules in the NIM to mimick the intact cytosol (Danker et al., 2001). Basically, we used 1.5% PVP, a concentration that prevents nuclear swelling, which instantaneously occurs during isolation in pure electrolyte solution. We compared the passive macromolecule permeability of nuclei tested in absence and in presence of PVP. For direct comparison of the results (± PVP) we considered the 4.1-times larger volume of the cell nuclei exposed to PVP-free NIM.

Application of gp62 Antibody

The polyclonal antibody directed against nucleoporin gp62 was a kind gift of G. Krohne (Biocentre, University of Würzburg, Germany). It is specific to *X. laevis* gp62 (Cordes, Waizenegger & Krohne, 1991). Nuclei were incubated for 1 h in NIM containing the antibody (1:250 dilution of the serum).

Stage-II and Stage-VI Oocytes

The oocyte development is classified in to six different stages (Dumont, 1972). Oocyte size dramatically increases from early to late stages in oocyte development. A comparison of the initial slope of nuclei from different stages and thus different sizes is only meaningful when surface/volume ratios are taken into consideration. While the surface of a sphere increases with the square of its radius ($4\pi r^2$), the volume increases with its cube radius ($4/3\pi r^3$). Furthermore, NIM used for this experimental series contained a Ca^{2+} concentration of 10^{-8} M and no ATP. To compare the permeability of nuclei from different developmental stages, we chose a PVP concentration of 0.5% because handling, measurement and analysis of slightly volume-expanded nuclei of small size are more easily performed.

Principle of the Measurement

Macromolecule permeability of cell nuclei was measured with fluorescence-labeled dextran of defined size using confocal fluorescence microscopy. The light source of the confocal laser-scanning microscope (CLSM Fluoview, Olympus) was an argon/crypton ion laser (Omnichrome®), which generates three excitation wavelengths, 488, 568 and 647 nm.

The underlying principle of exploring passive transport of macromolecules is that a change in NPC regulatory factors is followed by a change in the passive diffusion rate of fluorescence-labeled dextran. Comparison of diffusion rates under different experimental conditions allows conclusions about NPC permeability.

During the measurement the nucleus was placed in a superfusion chamber (volume: 100 μl), which, in combination with a perfusor, allows permanent superfusion and fast changes in perfusion solutions. To prevent the nucleus from moving, it was kept in place by using Cell-tak®.

Dextran molecules can move freely between cytoplasm and nucleus up to a size of ~20–40 kD (Peters, 1986). Therefore, we

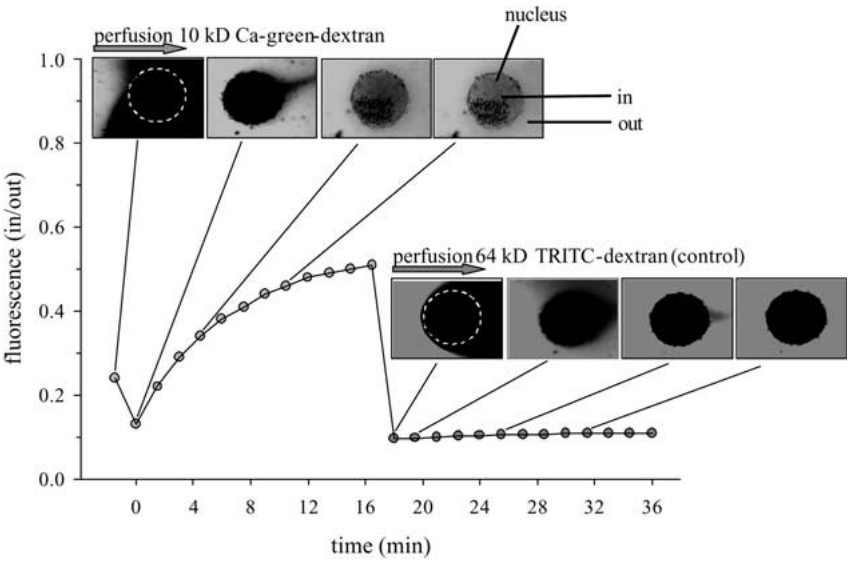

Fig. 1. Representative experiment of an individual nucleus. The graph represents the time course of an experiment. The fluorescence ratio (internal/external) is given on the *y*-axis. Images show the nucleus exposed to 10-kD Ca-Green-dextran and, subsequently, to 64-kD TRITC-dextran. 64-kD dextran was used to test for overall NE integrity.

used 10-kD dextran (highly permeable) to test for the NPC diffusional pathway and 64-kD dextran (virtually impermeable) to check for overall integrity of the nucleus. The 'small dextrans' (10 kD) were labeled with either FITC (fluoresceine isothiocyanate; Sigma) or with Calcium Green (Molecular Probes). The results obtained with these two differently labeled dextrans are not directly comparable because they require different laser adjustments and differ in sensitivity. The 'control dextrans' (64 kD) were marked with TRITC (tetramethylrhodamine isothiocyanate). Dependent upon the fluorescent dye, we used excitation wavelengths of 488 nm (FITC, Calcium Green) or 568 nm (TRITC). This strategy allowed us to test the integrity of each nucleus after a successful measurement with 10-kD dextran. The concentration of fluorescence-labeled dextran in the superfusion was 0.01 mM.

A representative experiment is shown in Fig. 1. The measurement starts with 10-kD dextran. After the start of perfusion, the nucleus is scanned 12 times every 90 seconds. Subsequently, the membrane integrity of the nucleus is tested by using the 64-kD dextran. To evaluate the fluorescence quantitatively, we determined nuclear and bath fluorescence intensity of each scanned image. Each fluorescence-intensity value of the nucleus was related to bath fluorescence intensity at the same time. The initial slope was derived from the straight line set through the first three test points. The initial slope directly correlates with macromolecule NE permeability.

Atomic Force Microscopy

Preparation of the NE for AFM was performed in NIM containing no PVP. Individual intact nuclei were transferred to a glass coverslip placed under a stereo microscope. The chromatin was carefully removed using sharp needles and the NE was spread on Cell-tak®-coated glass, with the nucleoplasmic side facing upward. Finally, the preparation was washed with deionized water and dried. No fixatives were used.

Application of AFM to nuclear envelopes has been described in detail previously (Danker, T. et al. 1997). We used a BioScope™ (with a NanoScope IIIa controller; Digital Instruments, Santa Barbara, CA). We used standard V-shaped 200 μm long silicium nitride cantilevers with spring constants of 0.06 N/m (VEECO, Mannheim, Germany). The images were recorded with 512 lines per screen at constant force (height mode) in contact mode with a scan rate of 3 to 10 Hz and analyzed with software supplied by the manufacturer (Digital Instruments).

Statistics

Data are shown as mean values ± SEM (n = number of nuclei). Significance of differences was tested by paired and unpaired Student's t-test, as appropriate. An asterisk indicates a significant difference of $p < 0.05$ or less.

Results

No Influence of Ca^{2+} and ATP on Macromolecule NE Permeability

To test the influence of the filling state of the perinuclear Ca^{2+} store on NE permeability we applied conditions in which the Ca^{2+} store was assumed to be empty. We compared the results of these measurements with the corresponding controls. Independently of the methods used to deplete the Ca^{2+} store (*see* Methods section), we could not measure a difference in 10-kD FITC-dextran permeability compared to controls. A typical experimental series is shown in Fig. 2. It is obvious that the initial slope did not significantly vary whether Ca^{2+} and ATP were present or absent. In the presence of Ca^{2+} and ATP the initial slope was 0.024 ± 0.0018 (mean ± SEM; n = 13). Omission of Ca^{2+} and ATP displayed an initial slope of 0.027 ± 0.0015 (mean ± SEM; n = 7). There is no significant difference of the mean values.

No Influence of Cytosolic pH on Macromolecule NE Permeability

To explore the influence of pH changes on the NE permeability, we tested nuclei under three different

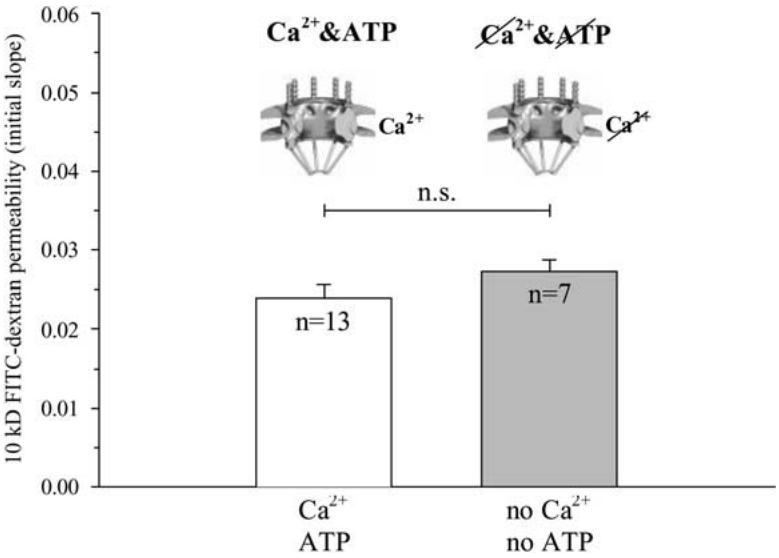

Fig. 2. The 10-kD FITC-dextran permeability of oocyte nuclei shown as initial slope of fluorescence-ratio increase in presence and absence of Ca^{2+} and ATP. Models above the columns show profiles through individual NPCs perpendicular to the NE, indicating the experimental condition. Cisternal Ca^{2+} stores are assumed to be empty in experiments where ambient Ca^{2+} and ATP were absent (n.s. = no significant difference).

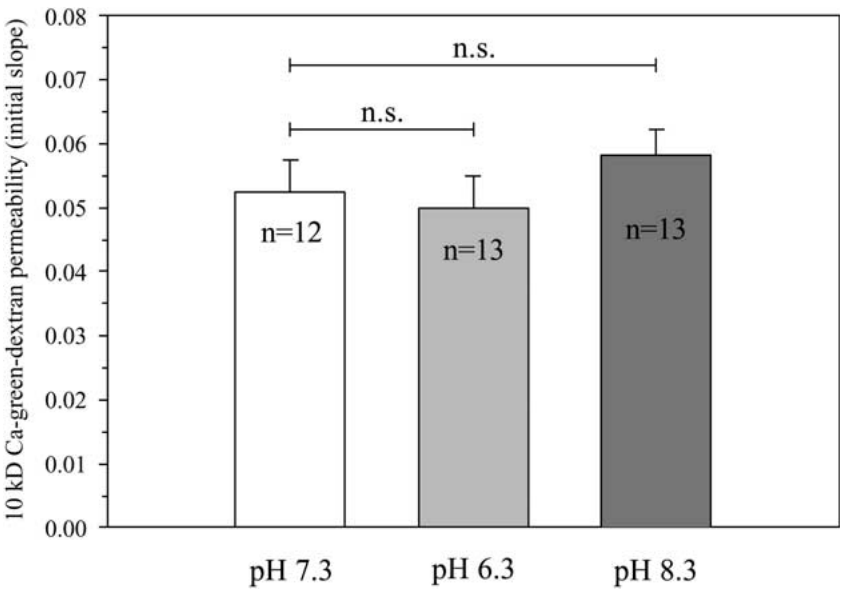

Fig. 3. 10-kD Ca-Green-dextran permeability of oocyte nuclei shown as initial slopes at different ambient pH.

pH values (7.3, 6.3 and 8.3). The results in Fig. 3 do not exhibit a significant difference between the three experimental groups. At physiological pH of 7.3 the permeability shown as initial slope was 0.053 ± 0.0049 (mean ± SEM; $n = 12$). The initial slope measured at pH of 6.3 was 0.050 ± 0.0050 (mean ± SEM; $n = 13$). Under the third condition, at pH of 8.3, oocyte nuclei exhibited an initial slope of 0.058 ± 0.0040 (mean ± SEM; $n = 13$). There is no significant difference of the mean values.

Dependence of Macromolecule NE Permeability on Nuclear Volume

After correction for surface/volume ratio (*see* Methods section) the initial slope of 12 nuclei tested in absence of PVP (volume-expanded state) was 0.028 ± 0.0027 (mean ± SEM; $n = 12$), as seen in Fig. 4. Initial slopes of ten nuclei measured in the presence of PVP were 0.007 ± 0.00045 (mean ± SEM; $n = 10$). Nuclei displayed a 4 times higher permeability for 10-kD FITC-dextran in the volume-expanded state compared to the permeability measured in the volume-contracted state ($p < 0.001$).

Dependence of Macromolecule NE Permeability on Central Channel Passage

Figure 5 shows the initial slope of 8 nuclei incubated with the nucleoporin gp62 antibody as compared to 14 nuclei that had no exposure to the antibody. After

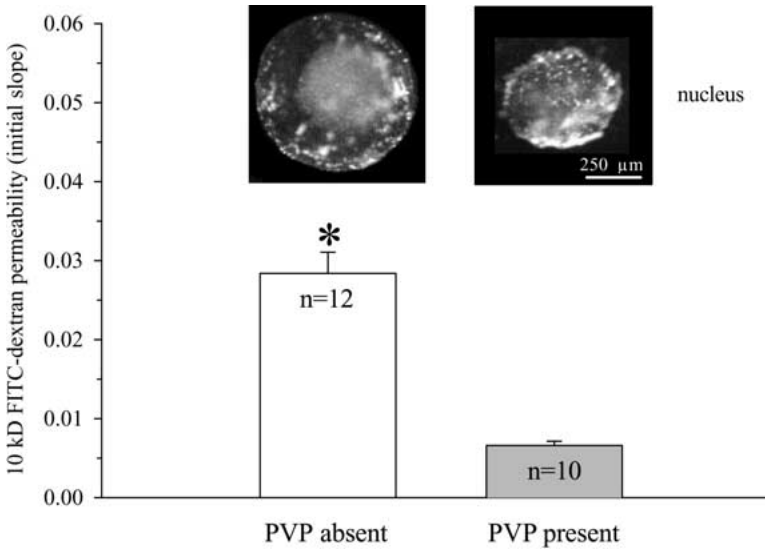

Fig. 4. 10-kD FITC-dextran permeability shown as initial slope in volume-expanded (PVP absent) and volume-contracted (1.5% PVP present) oocyte nuclei (*indicates $p < 0.01$).

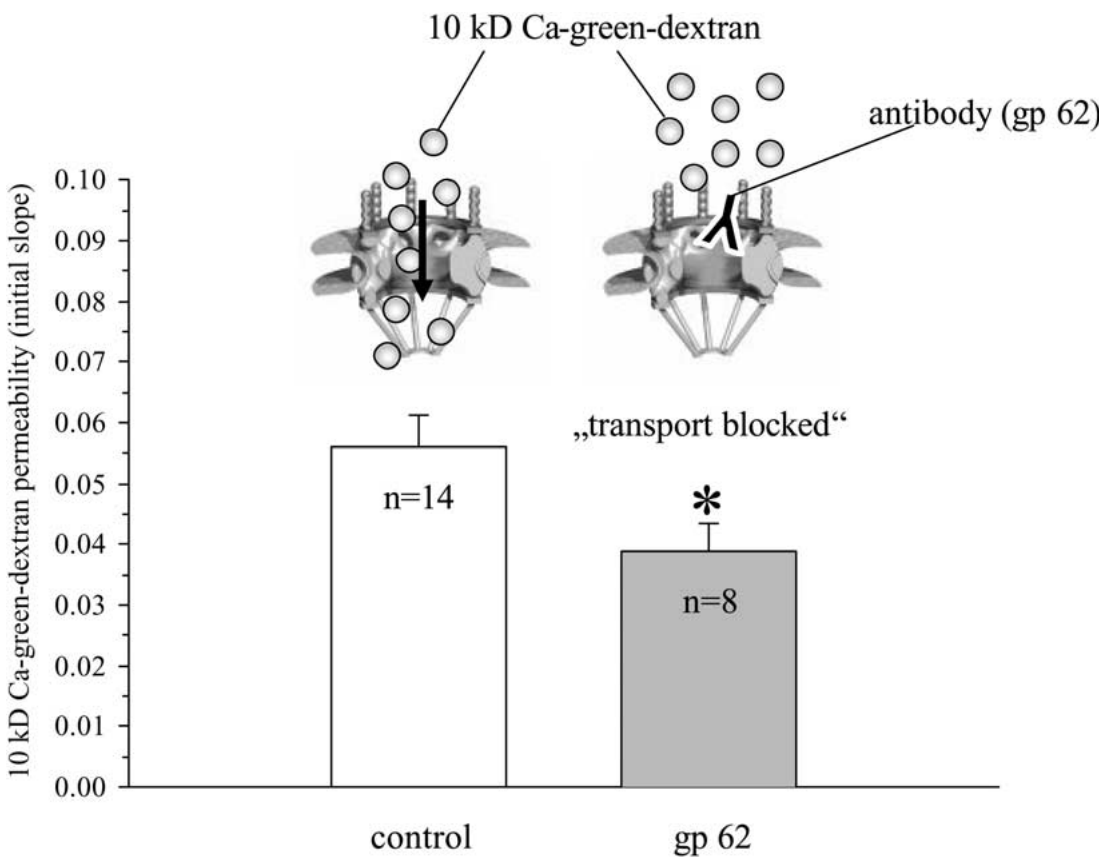

Fig. 5. 10-kD Ca-Green-dextran permeability shown as initial slope without (*control*) and with (*gp62*) antibody incubation. The NPC schematics above each column illustrate the experimental conditions (*indicates $p < 0.05$).

antibody treatment the initial slope for 10-kD Ca-Green-dextran with a value of 0.039 ± 0.0047 (mean ± SEM; $n = 8$) was significantly lower ($p < 0.05$) than that of the control nuclei with an initial slope of 0.056 ± 0.005 (mean ± SEM; $n = 14$).

Dependence of Macromolecule NE Permeability on Developmental Stages

In Fig. 6, results are shown after correction for different surface/volume ratios (*see* Methods) of stage-

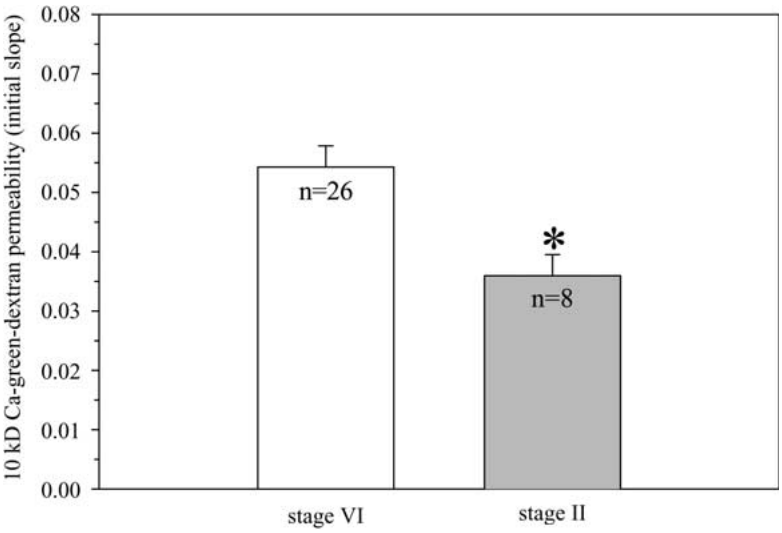

Fig. 6. 10 kD Ca-Green-dextran permeability shown as initial slope observed in stage-VI (late stage) and stage-II (early stage) *Xenopus laevis* oocytes (*indicates $p < 0.05$).

II and stage-VI oocyte nuclei. The initial slope for stage-VI nuclei was 0.054 ± 0.0035 (mean ± SEM; $n = 26$). The initial slope derived from stage-II nuclei was significantly lower, with a value of 0.036 ± 0.0036 (mean ± SEM; $n = 8$; $p < 0.01$). Thus, oocyte nuclei from early developmental stages are less permeable to 10-kD dextran than nuclei from stage-VI oocytes.

Plug Formation in Early and Late Developmental Stages

Figure 7 shows AFM images of NPCs obtained in early- and late-stage oocytes. While most of the NPCs appeared unplugged in the late stage, central channel plugging was clearly visible in early-stage oocytes. Profiles taken in individual NPCs showed plugs that occupy the central channels. Table 1 quantifies these observations. However, it should be mentioned that plugs are detectable only if they are located close to the NPC surface (here: nucleoplasmic surface). It is likely that plugs occur deeply inside the central channel, thus being undetectable for the AFM scanning tip.

Discussion

The fluorescence technique used in the present study has sufficient sensitivity and temporal resolution to measure diffusion rates in individual cell nuclei. The in-vitro system allows the examination of macromolecule NE permeability under controlled conditions. Control of overall nuclear integrity with 64-kD TRITC-dextran lowered the experimental scatter because damaged nuclei could be identified and excluded from analysis.

Ca^{2+} Does not Regulate the Passive Macromolecule Transport

The role of the filling state of the Ca^{2+} store concerning transport through NPCs is still unclear. There is evidence that passive transport is regulated by the filling state of the Ca^{2+} store (Stehno-Bittel, Perez-Terzic & Clapham, 1995). Furthermore, the state of the Ca^{2+} store is believed to influence NPC conformation (Perez-Terzic et al., 1996). Active transport of proteins and diffusion of small macromolecules was shown to decrease following the depletion of the Ca^{2+} store (Greber & Gerace, 1995; Perez-Terzic et al., 1999). The present data do not agree with previous measurements. This discrepancy could originate in different experimental approaches: While some researchers used living cells, we chose the isolated nuclei preparation. While we measured initial slopes, other researchers derived NE permeability from long-term incubations (Greber & Gerace, 1995). While we prevented nuclear swelling by adding PVP, other researchers measured NE permeability under volume-expanded conditions (Stehno-Bittel et al., 1995). This is also reflected by the use of nuclear ghosts, which presumably lack structural integrity. It is possible that a mechanically stressed cell nucleus could respond differently to Ca^{2+} depletion. Although there are reports in favor of our present study (Kasper et al., 1999), this issue is not yet resolved.

Interesting perspectives are provided by electrophysiological measurements. While NE macromolecule-permeability is not influenced by Ca^{2+}-store depletion (this study) passive NE ion-permeability, measured with electrophysiological techniques, is Ca^{2+}- and ATP-sensitive (Shahin et al., 2001). This strongly indicates a separate route for the passive transport of macromolecules and inor-

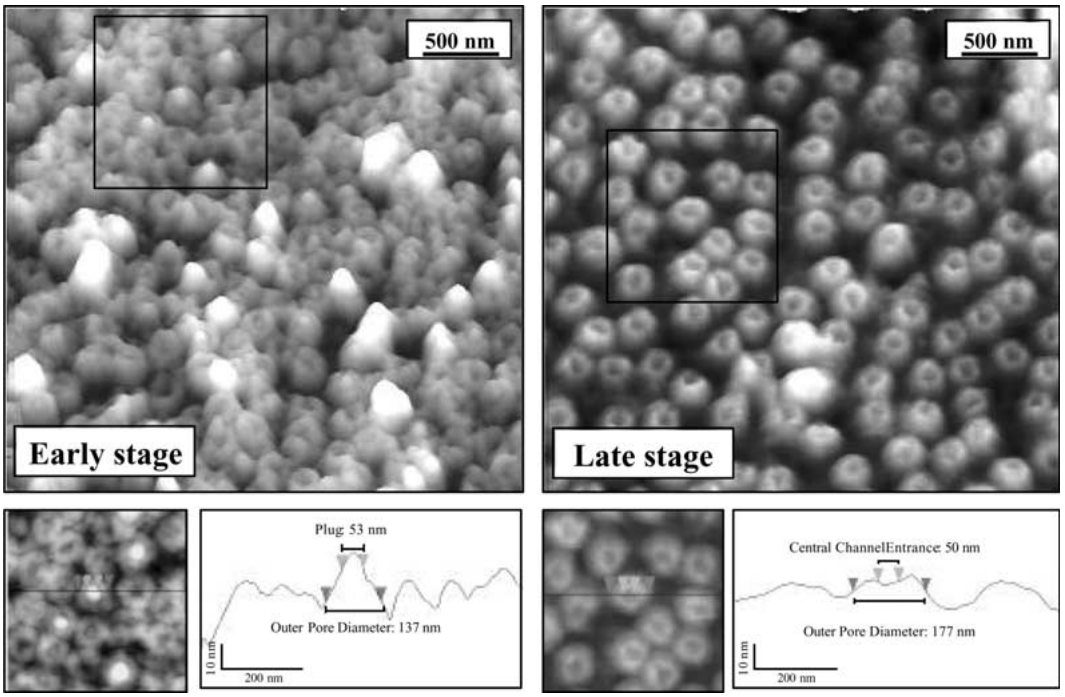

Fig. 7. Nuclear pore complexes of *X. laevis* oocyte nuclei imaged from the nucleoplasmic side with AFM. Incidence of plugged pores at the early stage of development is much higher (*left*) compared to plugging at the late stage of development. Top views and profile analysis of individual NPCs are shown in detail in the respective lower parts of the figure.

ganic ions, as previously suggested (Mazzanti et al., 2001).

10-kD Macromolecule Transport is Insensitive to Cytosolic pH

Cytoplasmic pH is usually well controlled within the range of pH 7.1 to pH 7.5. Little is known about pH in the perinuclear compartment, its regulation and its physiological role. Studies in intact cells show no changes of the NE macromolecule-permeability after acidification (Nitschke et al., 1996). The present experiments confirm this view. However, there is again a difference between ion and macromolecule permeability.

While passive transport of macromolecules is not influenced by pH changes, electrical NE conductance as well as NPC conformation strongly depend upon ambient pH (Danker & Oberleithner, 2000; Oberleithner et al., 2000a). This again indicates the existence of two separate transport routes.

Volume-expanded Nuclei Are More Permeable to 10-kD Dextran

Nuclear swelling is known to cause changes in NE ionic permeability (Innocenti & Mazzanti, 1993). It is obvious that volume-expanded nuclei are more permeable for both inorganic ions and macromolecules. This could be due to mechanical stress of the NE, although overall NE integrity remains intact. However, there is certainly mechanical stress upon the nuclear lamina and the individual NPCs, which could cause an increase in NE permeability. In addition, the chromatin appears detached from the NE as viewed in the light microscope, indicating that nuclear volume expansion, due to the lack of cytosolic marcomolecules (or PVP), structurally changes the nuclear compartment.

Antibody against Nucleoporin gp62 Interferes with Macromolecule Movement

Macromolecule diffusion is basically influenced by the size of the diffusing particle and the size of the diffusion pore. The gp62 antibody binds to the inside of the NPC central channel and thus physically inhibits passive diffusion.

Although gp62 is essential for active (Finlay et al., 1991; Hu et al., 1996) and passive transport of macromolecules, it is notable that the same antibody did not affect passive transport of ions (Danker et al., 1999). Again, this is strong evidence that macromolecule and ion pathways represent separate routes.

Table 1. NPC-data in early stage-II and late stage-VI *Xenopus laevis* oocytes obtained with atomic force microscopy

Parameter	Stage II		Stage VI	
	Data	*n*	Data	*n*
Number of NPCs/nucleus	10,064,000 ± 29,000	8	52,147,800 ± 125,000	18
Number of NPCs/μm^2 of nuclear envelope	36.2 ± 0.9	8	26.1 ±1.6	18
Number of plugged NPCs/nucleus	825,000		469,000	
Number of plugged NPCs/total number of NPCs (%)	8.2 ± 1.6	12	0.9 ± 1.6*	5

Mean values ± SEM. NPCs = nuclear pore complexes; total NPCs = total number of NPCs per respective area, n = number of nuclei. A total area per nucleus of about 500 μm^2 was analyzed. Asterisk indicates significantly different from the corresponding mean value of stage-II oocytes ($p < 0.02$). Plugged NPCs/nucleus are estimates taken from atomic force microscopy images.

NE Macromolecule Transport in Oocyte Development

Nuclei of early developmental stages are significantly less permeable for macromolecules compared to nuclei of late stages. An answer can be derived from AFM structural analysis (Table 1). Obviously, the NE macromolecule-permeability cannot be directly related to the number of pores per area. If it is assumed that NE macromolecule-permeability of stage-VI nuclei equals 100%, then a reduced permeability of 48% for stage-II nuclei is calculated, taking into consideration differences in nuclear size and NPC number. Thus, structural and functional changes of NPCs themselves must be assumed to explain the shift in permeability. Transcription activity is high in early-stage oocytes and low in late-stage oocytes (Dumont, 1972; Golden, Schafer & Rosbash, 1980). In early stages of development, huge amounts of ribonucleoproteins (RNPs) are actively transported from the nucleus into the cytoplasm. AFM is able to disclose RNPs in transit through individual NPCs (Schafer et al., 2002). Ribonucleoproteins form large plugs that obviously reduce the passive transport of macromolecules. Indeed, the number of plugged pores is much higher in early than in late stages of oocyte development. It is 8.2% in stage-II and only 0.9% in stage-VI oocyte nuclei. It is important to note that the number of plugged pores is probably underestimated due to technical reasons. AFM detects plugs only if they are located close to the NPC surface. However, the length of the NPC central channel is about 70 nm (Gerace & Burke, 1988; Pante & Aebi, 1993) and thus can hide several RNPs in a row. This view agrees with electrophysiological measurements. Ion flux is reduced during translocation of transcription factors (Bustamante et al., 1995a), macromolecules (Bustamante et al., 1995b) and RNPs (Schafer et al., 2002). The fact that ion flux through NPCs is reduced when RNPs are transported does not contradict the model of two separate pathways, one for the macromolecule and another for ions. As obvious from AFM studies, RNP transport through NPCs dramatically dilates the NPC ring-structure (Schafer et al., 2002). Thus, the small peripheral channels located in the ring are likely to be squeezed. This could explain the reduction of ion flow through NPCs when large macromolecules enter or exit the nucleus.

In conclusion, the data confirm the model that the NPC central channel transports the macromolecules, while peripheral channels transport the inorganic ions.

We thank Prof. G. Krohne, University of Würzburg, Germany, for the generous gift of gp62 antibody. We gratefully acknowledge the excellent technical assistance of Marianne Wilhelmi and Hannelore Arnold. The project was supported by grants of the Volkswagenstiftung (Project BD 151103) and the Interdisziplinäres Klinisches Forschungszentrum (IZKF Project A9).

References

Aebi, U., Pante, N., Jarnik, M. 1992. Structure and function of the nuclear pore complex, a supramolecular machine mediating molecular trafficking across the nuclear envelope. *Verh. Dtsch. Zool. Ges.* **85:**285–296

Bustamante, J.O., Hanover, J.A., Liepins, A. 1995b. The ion channel behavior of the nuclear pore complex. *J. Membrane Biol.* **146:**239–251

Bustamante, J.O., Oberleithner, H., Hanover, J.A., Liepins, A. 1995a. Patch clamp detection of transcription factor translocation along the nuclear pore complex channel. *J. Membrane Biol.* **146:**253–261

Cordes, V., Waizenegger, I., Krohne, G. 1991. Nuclear pore complex glycoprotein p62 of *Xenopus laevis* and mouse: cDNA cloning and identification of its glycosylated region. *Eur. J. Cell Biol.* **55:**31–47

Danker, T., Mazzanti, M., Tonini, R., Rakowska, A., Oberleithner, H. 1997. Using atomic force microscopy to investigate patch clamped nuclear membrane. *Cell Biol. Int.* **2111:**747–757

Danker, T., Oberleithner, H. 2000. Nuclear pore function viewed with atomic force microscopy. *Pfluegers Arch.* **439:**671–681

Danker, T., Schillers, H., Storck, J., Shahin, V., Kramer, B., Wilhelmi, M., Oberleithner, H. 1999. Nuclear hourglass technique: an approach that detects electrically open nuclear pores in *Xenopus laevis* oocyte. *Proc. Natl. Acad. Sci. USA* **96:**13530–13535

Danker, T., Shahin, V., Schlune, A., Schafer, C., Oberleithner, H. 2001. Electrophoretic plugging of nuclear pores by using the nuclear hourglass technique. *J. Membrane Biol.* **184:**91–99

Dumont, J.N. 1972. Oogenesis in *Xenopus laevis* (Daudin). I Stages of oocyte development in laboratory maintained animals. *J. Morphol.* **136:**153–179

Finlay, D.R., Meier, E., Bradley, P., Horecka, J., Forbes, D.J. 1991. A complex of nuclear pore proteins required for pore function. *J. Cell Biol.* **114:**169–183

Gerace, L., Burke, B. 1988. Functional organization of the nuclear envelope. *Annu. Rev. Cell Biol.* **4:**335–374

Golden, L., Schafer, U., Rosbash, M. 1980. Accumulation of individual pA+ RNAs during oogenesis of *Xenopus laevis*. *Cell* **22:**835–844

Greber, U.F., Gerace, L. 1995. Depletion of calcium from the lumen of endoplasmic reticulum reversibly inhibits passive diffusion and signal-mediated transport into the nucleus. *J. Cell Biol.* **128:**5–14

Guan, T., Muller, S., Klier, G., Pante, N., Blevitt, J.M., Haner, M., Paschal, B., Aebi, U., Gerace, L. 1995. Structural analysis of the p62 complex, an assembly of O-linked glycoproteins that localizes near the central gated channel of the nuclear pore complex. *Mol. Biol. Cell* **6:**1591–1603

Hinshaw, J.E., Carragher, B.O., Milligan, R.A. 1992. Architecture and design of the nuclear pore complex. *Cell* **69:**1133–1141

Hu, T., Guan, T., Gerace, L. 1996. Molecular and functional characterization of the p62 complex, an assembly of nuclear pore complex glycoproteins. *J. Cell Biol.* **134:**589–601

Innocenti, B., Mazzanti, M. 1993. Identification of a nucleo-cytoplasmic ionic pathway by osmotic shock in isolated mouse liver nuclei. *J. Membrane Biol.* **131:**137–142

Kasper, T., Ricken, S., Greger, R., Nitschke, R. 1999. The nuclear pore permeability is not regulated by the filling state of the intracellular Ca^{2+} stores or the cytosolic Ca^{2+} activity in HeLa and HT_{29} cells. *Pfluegers Arch.* **437:**11

Loewenstein, W.R., Kanno, Y. 1963. Some electrical properties of a nuclear membrane examined with a microelectrode. *J. Gen. Physiol.* **46:**1123–1140

Mazzanti, M., Bustamante, J.O., Oberleithner, H. 2001. Electrical dimension of the nuclear envelope. *Physiol. Rev.* **81:**1–19

Mazzanti, M., DeFelice, L.J., Cohn, J., Malter, H. 1990. Ion channels in the nuclear envelope. *Nature* **343:**764–767

Mazzanti, M., Innocenti, B., Rigatelli, M. 1994. ATP-dependent ionic permeability on nuclear envelope in in situ nuclei of *Xenopus* oocytes. *FASEB J.* **8:**231–236

Nitschke, R., Riedel, A., Ricken, S., Leipziger, J., Benning, N., Fischer, K.G., Greger, R. 1996. The effect of intracellular pH on cytosolic Ca^{2+} in HT_{29} cells. *Pfluegers Arch.* **433:**98–108

Oberleithner, H., Reinhardt, J., Schillers, H., Pagel, P., Schneider, S.W. 2000b. Aldosterone and nuclear volume cycling. *Cell Physiol. Biochem.* **10:**429–434

Oberleithner, H., Schafer, C., Shahin, V., Schlune, A., Schillers, H., Reinhardt, J. 2001. Nuclear plug harvesting using atomic force microscopy. *Single Molecules* **2:**117–120

Oberleithner, H., Schillers, H., Wilhelmi, M., Butzke, D., Danker, T. 2000a. Nuclear pores collapse in response to CO_2 imaged with atomic force microscopy. *Pfluegers Arch.* **439:**251–255

Pante, N., Aebi, U. 1993. The nuclear pore complex. *J. Cell Biol.* **22:**977–984

Perez-Terzic, C., Gacy, A.M., Bortolon, R., Dzeja, P.P., Puceat, M., Jaconi, M., Prendergast, F.G., Terzic, A. 1999. Structural plasticity of the cardiac nuclear pore complex in response to regulators of nuclear import. *Circ. Res.* **84:**1292–1301

Perez-Terzic, C., Pyle, J., Jaconi, M., Stehno-Bittel, L., Clapham, D.E. 1996. Conformational states of the nuclear pore complex induced by depletion of nuclear Ca^{2+} stores. *Science* **273:**1875–1877

Peters, R. 1986. Fluorescence microphotolysis to measure nucleo-cytoplasmic transport and intracellular mobility. *Biochim. Biophys. Acta* **864:**305–359

Rakowska, A., Danker, T., Schneider, S.W., Oberleithner, H. 1998. ATP-Induced shape change of nuclear pores visualized with the atomic force microscope. *J. Membrane Biol.* **163:**129–136

Schafer, C., Shahin, V., Albermann, L., Hug, M.J., Reinhardt, J., Schillers, H., Schneider, S.W., Oberleithner, H. 2002. Aldosterone signaling pathway across the nuclear envelope. *Proc. Natl. Acad. Sci. USA* **99:**7154–7159

Shahin, V., Danker, T., Enss, K., Ossig, R., Oberleithner, H. 2001. Evidence for Ca^{2+}- and ATP-sensitive peripheral channels in nuclear pore complexes. *FASEB J.* **15:**1895–1901

Stehno-Bittel, L., Perez-Terzic, C., Clapham, D.E. 1995. Diffusion across the nuclear envelope inhibited by depletion of the nuclear Ca^{2+} store. *Science* **270:**1835–1838